Facile synthesis of anhydrous alkaline earth metal dodecaborates MB$_{12}$H$_{12}$ (M = Mg, Ca) from M(BH$_4$)$_2$†

Liqing He,[a] Hai-Wen Li,*[b,c] Nikolay Tumanov,[d] Yaroslav Filinchuk[d] and Etsuo Akiba[a,b,c]

Metal dodecaborates M$_{2/n}$B$_{12}$H$_{12}$ are among the dehydrogenation intermediates of metal borohydrides M(BH$_4$)$_n$ with a high hydrogen density of approximately 10 mass%, the latter is a potential hydrogen storage material. There is therefore a great need to synthesize anhydrous M$_{2/n}$B$_{12}$H$_{12}$ in order to investigate the thermal decomposition of M$_{2/n}$B$_{12}$H$_{12}$ and to understand its role in the dehydrogenation and rehydrogenation of M(BH$_4$)$_n$. In this work, anhydrous alkaline earth metal dodecaborates MB$_{12}$H$_{12}$ (M = Mg, Ca) have been successfully synthesized by sintering M(BH$_4$)$_2$ (M = Mg, Ca) and B$_{10}$H$_{14}$ in a stoichiometric molar ratio of 1 : 1. Thermal decomposition of MB$_{12}$H$_{12}$ shows multistep pathways with the formation of H-deficient monomers MB$_{12}$H$_{12-x}$ containing icosahedral B$_{12}$ skeletons and is followed by the formation of (MB$_y$H$_z$)$_n$ polymers. Comparison of the thermal decomposition of MB$_{12}$H$_{12}$ and M(BH$_4$)$_2$ suggests different behaviours of the anhydrous MB$_{12}$H$_{12}$ and those formed from the decomposition of M(BH$_4$)$_n$.

1. Introduction

Hydrogen, known as an environmentally friendly energy carrier, can be stored in chemical materials in the form of hydrides. Among the various kinds of hydrides, borohydrides with high volumetric and gravimetric hydrogen densities such as LiBH$_4$ (H capacity: 18.5 mass% and 122 kg H$_2$ per m^3), Mg(BH$_4$)$_2$ (14.9 mass% and 147 kg H$_2$ per m^3) and Ca(BH$_4$)$_2$ (11.6 mass% and 124 kg H$_2$ per m^3) have been considered as potential hydrogen storage materials.[1–4] Most of the borohydrides show a stepwise decomposition accompanied by the formation of intermediates containing polyanions, such as [B$_2$H$_6$]$^{2-}$, [B$_3$H$_8$]$^-$ and/or [B$_{12}$H$_{12}$]$^{2-}$. The decomposition mechanism significantly depends on the dehydrogenation temperature and hydrogen backpressure as well as the particle size of the borohydrides.[5–17] The intermediates containing small clusters like [B$_2$H$_6$]$^{2-}$ and [B$_3$H$_8$]$^-$ were found to be beneficial for

^{a}Department of Mechanical Engineering, Faculty of Engineering, Kyushu University, Fukuoka 819-0395, Japan
^{b}International Research Center for Hydrogen Energy, Kyushu University, Fukuoka 819-0395, Japan. E-mail: li.haiwen.305@m.kyushu-u.ac.jp; Fax: +81-92-802-3235; Tel: +81-92-802-3226
^{c}WPI International Institute for Carbon-Neutral Energy Research (WPI-I2CNER), Kyushu University, Fukuoka 819-0395, Japan
^{d}Institute of Condensed Matter and Nanosciences, Université catholique de Louvain, Louvain-la-Neuve 1348, Belgium
†Electronic supplementary information (ESI) available: MS spectra of Mg(BH$_4$)$_2$, XRD patterns and Raman spectra of MgB$_{12}$H$_{12}$ and CaB$_{12}$H$_{12}$ heated to respective temperatures. See DOI: 10.1039/c5dt02343b

the rehydrogenation to the corresponding borohydrides.[13,16,18] The [B$_{12}$H$_{12}$]$^{2-}$ intermediate, despite the fact that its formation is still controversial, having strong B–B bonds in a stable icosahedral boron cage, has been widely regarded as an obstacle for the rehydrogenation to M(BH$_4$)$_n$.[7,10,19–21] Fundamental investigation on the thermal decomposition of metal dodecaborates M$_{2/n}$B$_{12}$H$_{12}$, therefore, is in great need to elucidate their role in the dehydrogenation and rehydrogenation of borohydrides.

M$_{2/n}$B$_{12}$H$_{12}$ is generally synthesized using wet chemistry processes, followed by careful dehydration under vacuum slightly above 120 °C.[22,23] Higher temperatures cause hydrolysis, and lower temperatures do not allow the removal of water completely, thus failing to synthesize some anhydrous alkaline earth metal dodecaborates such as MgB$_{12}$H$_{12}$.[24] Under such conditions, we have recently developed a novel solvent-free synthesis method, *i.e.* sintering of M(BH$_4$)$_n$ with B$_{10}$H$_{14}$, by which high purity anhydrous alkali metal dodecaborates M$_2$B$_{12}$H$_{12}$ (M = Li, Na, K) have been successfully synthesized.[25]

In this work, we have applied our recently developed sintering process to the syntheses of anhydrous alkaline earth metal dodecaborates MgB$_{12}$H$_{12}$ and CaB$_{12}$H$_{12}$. Anhydrous MB$_{12}$H$_{12}$ have been successfully synthesized by sintering Mg(BH$_4$)$_2$ and Ca(BH$_4$)$_2$ with B$_{10}$H$_{14}$, based on eqn (1):

$$M(BH_4)_2 + B_{10}H_{14} \rightarrow MB_{12}H_{12} + 5H_2 \ (M = Mg, Ca) \quad (1)$$

Thermal decomposition behaviours of the thus synthesized anhydrous MgB$_{12}$H$_{12}$ and CaB$_{12}$H$_{12}$ were carefully investigated

using thermogravimetry (TG), mass spectrometry (MS), X-ray diffraction (XRD), Raman spectroscopy and solid-state magic angle spinning (MAS) nuclear magnetic resonance (NMR) spectroscopy. Furthermore, the decomposition processes of $MgB_{12}H_{12}$ and $CaB_{12}H_{12}$ are compared with those for products formed during the dehydrogenation of $Mg(BH_4)_2$ and $Ca(BH_4)_2$, in order to elucidate their roles in the dehydrogenation of borohydrides.

2. Experimental

Commercial $B_{10}H_{14}$ (99%, Wako), γ-$Mg(BH_4)_2$ (95%, Aldrich) and $Ca(BH_4)_2$ (95%, Aldrich) were all stored in a glove box under Ar gas and used without further purification. Starting materials $Mg(BH_4)_2$ + $B_{10}H_{14}$ and $Ca(BH_4)_2$ + $B_{10}H_{14}$ were firstly mechanically milled at room temperature using a planetary ball mill (Fritsch P-7) with 10 steel balls (7 mm in diameter) in a hardened steel vial (30 cm^3 in volume) under 0.1 MPa Ar for 5 h (15 min milling, 5 min pausing). Subsequently, the ball milled samples of $Mg(BH_4)_2$ + $B_{10}H_{14}$ and $Ca(BH_4)_2$ + $B_{10}H_{14}$ were sealed into stainless steel crucibles for sintering at 300 °C for 1 h and at 380 °C for 2 h, respectively.

Powder XRD patterns were recorded by using a Rigaku Ultima IV X-ray diffractometer with Cu-Kα radiation, and the accelerating voltage/tube current were set as 40 kV/40 mA. The sample powders were placed on a glass plate sealed by using Scotch tape to prevent exposure to air during the measurement. Powder XRD patterns of the as-synthesized $MgB_{12}H_{12}$ were measured in a glass capillary, on a MAR345 diffractometer, with a Mo Kα rotating anode generator and a focusing mirror. The synchrotron radiation powder XRD pattern for the as-synthesized $CaB_{12}H_{12}$ was obtained on the Materials Science Beamline X04SA at the Swiss Light Source (transmission geometry in capillary, MYTHEN detector, λ = 1.00117 Å). A variable temperature experiment on the sample of $CaB_{12}H_{12}$ was carried out at the Materials Science Beamline X04SA, SLS, using a wavelength of 0.77619 Å. The sample was loaded in a glass capillary, and was heated in 20 °C steps from room temperature to 400 °C, and then cooled down to ambient temperature. A number of diffraction patterns were collected at each temperature point to follow both time and temperature dependences of the transformations.

Raman spectra were obtained from a RAMAN-11 VIS-SS (Nanophoton) using a green laser with 532 nm wavelength. Thermal decomposition was examined by TG with a heating rate of 5 °C min^{-1} under a 200 ml min^{-1} flow of He gas. The gas released during the TG measurement was analysed by using a quadrupole mass spectrometer coupled with TG. Solid-state MAS NMR spectra were recorded using a Bruker Ascend-600 spectrometer at room temperature. NMR sample preparations were always conducted in a glove box filled with purified Ar gas and dry N_2 gas was used for sample spinning. ^{11}B MAS NMR spectra were obtained at excitation pulses of 6.5 μs ($\pi/2$ pulse) and with strong ^1H decoupling pulses. ^{11}B NMR chemical shifts were referenced to BF_3·Et_2O (δ = 0.00 ppm).

3. Results and discussion

3.1. Synthesis of anhydrous $MgB_{12}H_{12}$ and $CaB_{12}H_{12}$

Fig. 1 shows the XRD pattern and Raman spectra of $Mg(BH_4)_2$ + $B_{10}H_{14}$ after sintering at 300 °C for 1 h. The observed broad peak between 2θ = 3° and 15° (between 2θ = 10° and 18° using Cu-Kα radiation as shown in Fig. S1†) is distinct from the starting materials $Mg(BH_4)_2$ and $B_{10}H_{14}$, as well as the amorphous $Mg(BH_4)_2$,[26] and could be ascribed to the formation of amorphous $MgB_{12}H_{12}$ theoretically predicted by first-principles calculations.[27] In the Raman spectra, two peaks ascribed to B–H bending and stretching vibrations of $[B_{12}H_{12}]^{2-}$ are observed at 751 and 2569 cm^{-1}, respectively, together with the high level of the baseline due to the fluorescence effect. Furthermore, no trace of the O–H bond of water is observed in the Raman spectra, which proves the successful synthesis of the anhydrous $MgB_{12}H_{12}$.

Anhydrous $CaB_{12}H_{12}$ is also synthesized by sintering $Ca(BH_4)_2$ + $B_{10}H_{14}$ at 380 °C for 2 h, and its XRD and Raman data are shown in Fig. 2. Three representative diffraction peaks at 2θ = 9.3°, 9.5° and 10.5° originating from $CaB_{12}H_{12}$ with a monoclinic ($C2/c$) crystal structure[28] are clearly observed in the XRD patterns. An impurity with an unknown structure was indexed in the orthorhombic crystal system (a = 13.580(2),
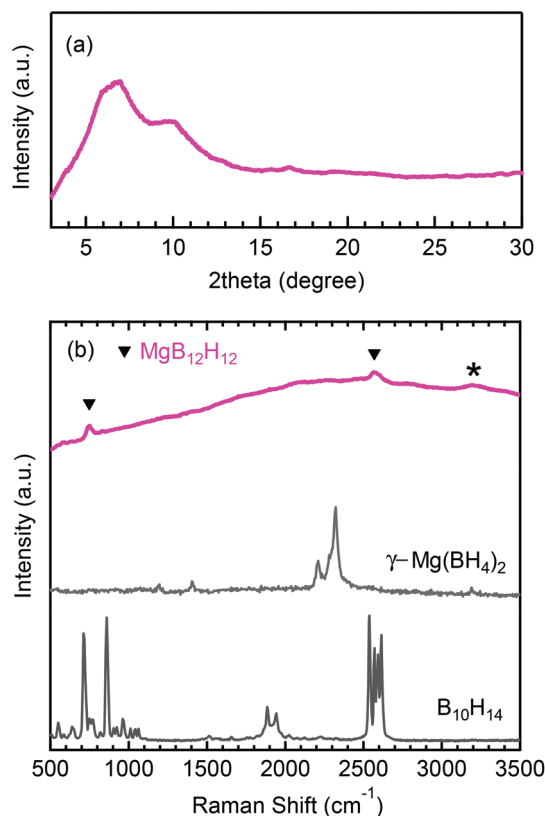

Fig. 1 (a) XRD pattern (Mo Kα) and (b) Raman spectra of 5 h ball milled $Mg(BH_4)_2$ + $B_{10}H_{14}$ followed by sintering at 300 °C for 1 h. Starting materials of $Mg(BH_4)_2$ and $B_{10}H_{14}$ are also shown as references, the asterisk indicates the systematic error.
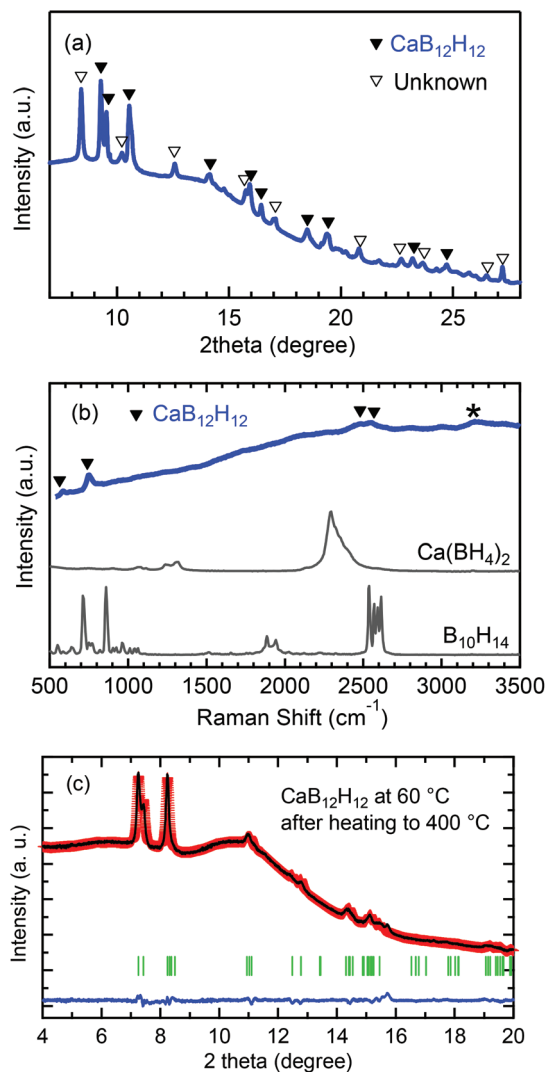
Fig. 2 (a) Synchrotron XRD (λ = 1.00117 Å) pattern and (b) Raman spectra of 5 h ball milled Ca(BH$_4$)$_2$ + B$_{10}$H$_{14}$ followed by sintering at 380 °C for 2 h. The asterisk indicates the systematic error. (c) Rietveld refinement plot for CaB$_{12}$H$_{12}$ at 60 °C after heating to 400 °C. The red crosses and black line show the experimental and calculated data, respectively. The blue line is the difference profile, and green marks indicate Bragg positions of CaB$_{12}$H$_{12}$.

Fig. 3 ^{11}B MAS NMR spectra of the synthesized samples from M(BH$_4$)$_2$ + B$_{10}$H$_{14}$ (M = Mg: 5 h ball milling followed by sintering at 300 °C for 1 h; M = Ca: 5 h ball milling followed by sintering at 380 °C for 2 h).

−26.3 ppm for Ca),[8,30] [BH$_4$]$^-$ (−41.9 ppm for Mg, −32.2 ppm for Ca)[27] and unknown phases (−6.0 and −46.3 ppm) are detected in the synthesized MgB$_{12}$H$_{12}$ and CaB$_{12}$H$_{12}$ samples as impurities. In addition, the synthesized anhydrous MgB$_{12}$H$_{12}$ and CaB$_{12}$H$_{12}$ samples display a homogeneous yellow color, which is different from the white starting materials. All the above mentioned results, therefore, consistently indicate that sintering of metal borohydrides M(BH$_4$)$_2$ with B$_{10}$H$_{14}$ is a facile method to synthesize anhydrous alkaline earth metal dodecaborates.

3.2. Thermal decomposition of anhydrous MgB$_{12}$H$_{12}$ and CaB$_{12}$H$_{12}$

3.2.1. MgB$_{12}$H$_{12}$. Thermal decomposition behaviour of the anhydrous MgB$_{12}$H$_{12}$ examined by TG and MS is shown in Fig. 4. Only hydrogen is detected by MS, indicating that the weight loss upon heating is originated from the dehydrogena-
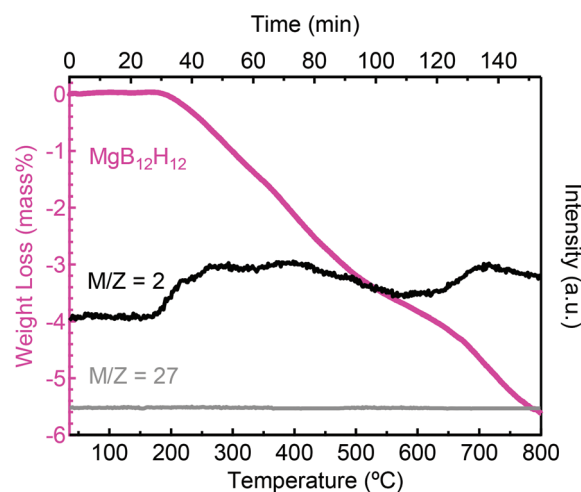
b = 12.264(1), c = 4.2495(4) Å) and our preliminary analysis suggests the space group symmetry *Pcab* or *Pbab*. Our *in situ* diffraction experiments show that the second crystalline phase disappears from the diffraction pattern after heating to 400 °C, see Fig. 2c. In Raman spectra, vibration peaks assigned to B–H bending and stretching modes of [B$_{12}$H$_{12}$]$^{2-}$ are observed at 585, 751 and 2485, 2547 cm^{-1}, respectively.[29] No O–H vibration peak of water is detected in Raman spectra, which indicates the successful synthesis of the anhydrous CaB$_{12}$H$_{12}$.

The successful syntheses of the anhydrous MgB$_{12}$H$_{12}$ and CaB$_{12}$H$_{12}$ are further proved from solid state ^{11}B MAS NMR spectra, as shown in Fig. 3. The main resonances at −15.0 and −14.0 ppm are assigned to [B$_{12}$H$_{12}$]$^{2-}$ in MgB$_{12}$H$_{12}$ and CaB$_{12}$H$_{12}$, respectively.[28] [B$_{10}$H$_{10}$]$^{2-}$ (−28.3 ppm for Mg,

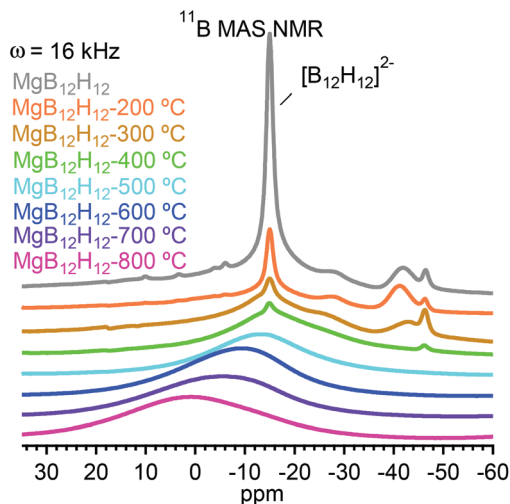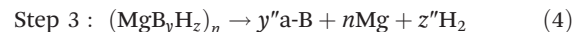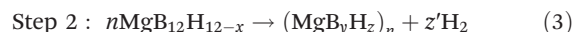Fig. 4 TG curve and MS signals of the synthesized MgB$_{12}$H$_{12}$ (mass numbers of 2 and 27 represent H$_2$ and B$_2$H$_6$).

Fig. 5 ^{11}B MAS NMR spectra of as-synthesized $MgB_{12}H_{12}$ and heated up to respective temperatures.

tion of $MgB_{12}H_{12}$. The dehydrogenation starts at approximately 190 °C, reaching 5.6 mass% or approximately 77% of the theoretical hydrogen content in $MgB_{12}H_{12}$ when heated up to 800 °C. The decomposition pathway is multistep, as shown by TG and MS results.

In order to elucidate the decomposition pathway of anhydrous $MgB_{12}H_{12}$, the sample was heated to fixed temperatures and subsequently cooled down to room temperature, and the changes were followed systematically by XRD, Raman and solid state ^{11}B NMR spectroscopy. The results are shown in Fig. S1† and Fig. 5, respectively. When the temperature is increased up to 200 °C, the main resonance at −15.0 ppm attributed to $MgB_{12}H_{12}$ becomes weak, while the peak intensity for $Mg(BH_4)_2$ and $MgB_{10}H_{10}$ impurities does not change obviously. This indicates that the decomposition of $MgB_{12}H_{12}$ starts at 190 °C, prior to that of $Mg(BH_4)_2$ as shown in Fig. S2.† When the temperature is increased up to 400 °C, the broad diffraction peak between $2\theta = 10°$ and 18° disappears, and the B–H stretching mode of $MgB_{12}H_{12}$ at 2569 cm^{-1} becomes almost invisible, and the main resonance of $MgB_{12}H_{12}$ at −15.0 ppm reduces significantly without any change in the chemical shift, which consistently indicate that a major part of the B–H bond in the icosahedral $[B_{12}H_{12}]^{2-}$ has been broken to release hydrogen. The released amount reaches 2.1 mass% at 400 °C, suggesting that the decomposition product is probably H-deficient $MgB_{12}H_{12-x}$ ($x = 3.5$) that retains the icosahedral B_{12} skeletons.[12] When the temperature is further increased to 500, 600 and 700 °C, the released amount of hydrogen reaches 3.2, 3.8 and 4.6 mass% and the major resonance of $[B_{12}H_{12}]^{2-}$ at −15.0 ppm shifts to −13.1, −9.4 and −5.6 ppm. It suggests that $MgB_{12}H_{12-x}$ continuously releases hydrogen accompanied by the polymerization of the icosahedral B_{12} skeletons and the formation of $(MgB_yH_z)_n$ polymers,[31,32] insoluble in water and DMSO. When the sample is heated up to 800 °C, the major resonance shifts to 0.9 ppm,

indicating the formation of amorphous boron (a-B) at 800 °C. The temperature is higher than that (600 °C) reported for $MgB_{12}H_{12}$/carbon nanocomposites,[33] suggesting that the carbon nanocomposite may contribute to the reduction of the decomposition temperature.

Based on the abovementioned experimental results, the thermal decomposition pathway of anhydrous $MgB_{12}H_{12}$ could be briefly summarized as the following steps:

$$\text{Step 1}: \ MgB_{12}H_{12} \rightarrow MgB_{12}H_{12-x} + x/2H_2 \quad (2)$$

$$\text{Step 2}: \ nMgB_{12}H_{12-x} \rightarrow (MgB_yH_z)_n + z'H_2 \quad (3)$$

$$\text{Step 3}: \ (MgB_yH_z)_n \rightarrow y''\text{a-B} + nMg + z''H_2 \quad (4)$$

It is worth emphasizing that the thermal decomposition behaviour of the synthesized $MgB_{12}H_{12}$ is fairly different from that formed during the dehydrogenation of $Mg(BH_4)_2$. The synthesized $MgB_{12}H_{12}$ exhibits a lower decomposition onset temperature and a wider decomposition temperature range of 190–800 °C than $Mg(BH_4)_2$. Also, the synthesized $MgB_{12}H_{12}$ decomposes into amorphous boron rather than MgB_2 formed as the decomposition product from $Mg(BH_4)_2$ at 600 °C.[34] Taking into account the controversial discussions about the formation of $MgB_{12}H_{12}$ during the dehydrogenation of $Mg(BH_4)_2$, these differences may result from the following two possibilities: (a) the concurrent formation of MgH_2 and $MgB_{12}H_{12}$ during the dehydrogenation of $Mg(BH_4)_2$, since MgH_2 facilitates the formation of MgB_2 from $MgB_{12}H_{12}$ as predicted by first-principles calculations;[9] and (b) $MgB_{12}H_{12}$ does not form as a stable dehydrogenation intermediate of $Mg(BH_4)_2$ as reported recently.[14]

3.2.2. $CaB_{12}H_{12}$. Thermal decomposition behaviour of anhydrous $CaB_{12}H_{12}$ is systematically studied and the TG and MS results are shown in Fig. 6. Only hydrogen is detected by MS, indicating that the weight loss upon heating comes from the dehydrogenation of $CaB_{12}H_{12}$. The dehydrogenation starts at *ca.* 320 °C and reaches 2.5 mass% (approximately 38% of the theoretical hydrogen capacity in $CaB_{12}H_{12}$), comparable to the reported value of 1.5 mass% at 600 °C.[28] The reaction has multiple steps when heated up to 750 °C.

The XRD patterns, Raman spectra and solid-state ^{11}B MAS NMR spectra of the anhydrous $CaB_{12}H_{12}$ heated to fixed temperatures and subsequently cooled down to room temperature are shown in Fig. S3† and Fig. 7, respectively. When $CaB_{12}H_{12}$ is heated up to 400 °C, no obvious changes of Raman spectra and the major resonance for $CaB_{12}H_{12}$ are seen, whereas the diffraction peaks of the unknown phase and the resonance at −32.2 ppm originate from the residual $Ca(BH_4)_2$ nearly disappearing at 375 °C. This indicates that the weight loss below 400 °C is responsible for the dehydrogenation of the residual $Ca(BH_4)_2$ and the unknown phase, suggesting that the impurities do not directly influence the decomposition of $CaB_{12}H_{12}$. When $CaB_{12}H_{12}$ is heated up to 500 °C, diffraction peaks and Raman spectra attributed to $CaB_{12}H_{12}$ disappear, the major resonance at −14.0 ppm becomes significantly weaker and overlaps with a broad resonance between 0 and −13 ppm,
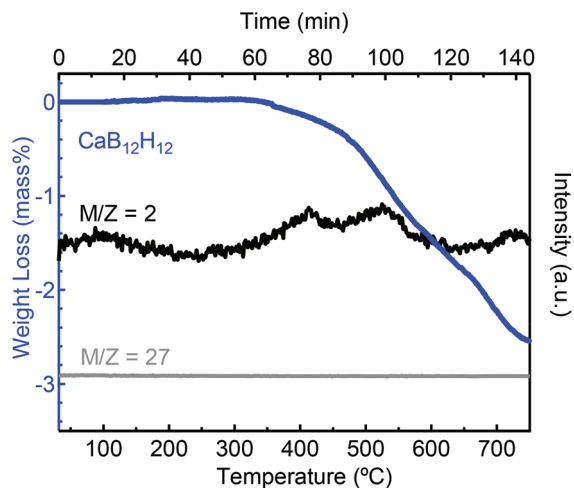
Fig. 6 TG curve and MS signals of the synthesized $CaB_{12}H_{12}$ (mass numbers of 2 and 27 represent H_2 and B_2H_6).

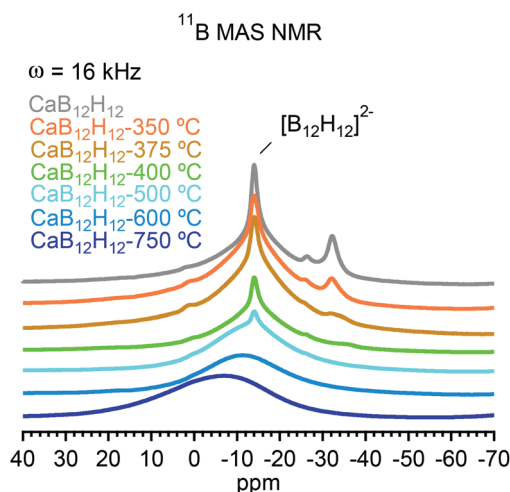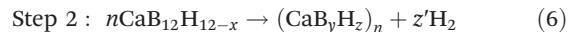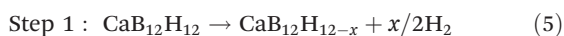**Fig. 7** ^{11}B MAS NMR spectra of as-synthesized $CaB_{12}H_{12}$ and heated up to respective temperatures.

suggesting that the dehydrogenation of $CaB_{12}H_{12}$ to $CaB_{12}H_{12-x}$ as well as a polymerization of $CaB_{12}H_{12-x}$ to water and DMSO insoluble $(CaB_yH_z)_n$ polymers starts close to 500 °C.[31,32] When $CaB_{12}H_{12}$ is further heated up to 600 °C and 750 °C, the major resonance shifts to −11.2 and −7.0 ppm, indicating the continuous polymerization of $(CaB_yH_z)_n$, similar to that of $MgB_{12}H_{12}$ heated up to 500–700 °C. Unlike $MgB_{12}H_{12}$, no obvious NMR spectrum originated from amorphous boron is observed when $CaB_{12}H_{12}$ is heated up to 750 °C, whereas CaB_6 has been demonstrated as the main dehydrogenation product of $Ca(BH_4)_2$ above 330 °C.[14,20,35]

The decomposition pathway of the anhydrous $CaB_{12}H_{12}$ is briefly summarized as the following steps (below 750 °C):

$$\text{Step 1}: \ CaB_{12}H_{12} \rightarrow CaB_{12}H_{12-x} + x/2H_2 \quad (5)$$

$$\text{Step 2}: \ nCaB_{12}H_{12-x} \rightarrow (CaB_yH_z)_n + z'H_2 \quad (6)$$

Similar to that of $MgB_{12}H_{12}$, the decomposition behaviour of the synthesized $CaB_{12}H_{12}$ does not seem to directly correlate with the dehydrogenation of $Ca(BH_4)_2$, suggesting that: (a) CaH_2 formed in the decomposition of $Ca(BH_4)_2$ facilitates the transformation of $CaB_{12}H_{12}$ to produce CaB_6 that is not detected when $CaB_{12}H_{12}$ is heated even up to 750 °C;[9,28] or (b) $CaB_{12}H_{12}$ does not form as a stable dehydrogenation intermediate of $Ca(BH_4)_2$ as reported recently.[16]

In summary, the thermal decomposition of $MgB_{12}H_{12}$ and $CaB_{12}H_{12}$ reveals two steps of (1) dehydrogenation to produce H-deficient $MB_{12}H_{12-x}$ and (2) polymerization of $MB_{12}H_{12-x}$ to form $(MB_yH_z)_n$, which is the main step to form amorphous boron, regarded as the major obstacle for rehydrogenation. The uncorrelated thermal decomposition behaviours of metal dodecaborates and metal borohydrides emphasize the importance of systematic investigations of various possible dehydrogenation intermediates and the corresponding metal borohydrides, in order to determine the exact dehydrogenation and rehydrogenation mechanisms for metal borohydrides.

4. Conclusions

Anhydrous alkaline earth metal dodecaborates $MgB_{12}H_{12}$ and $CaB_{12}H_{12}$ have been successfully synthesized through sintering of ball milled $M(BH_4)_2$ + $B_{10}H_{14}$ (M = Mg, Ca). This study again proves that sintering of borohydrides with $B_{10}H_{14}$ is a facile method to synthesize anhydrous metal dodecaborates. Systematic investigations of thermal decomposition demonstrate that both $MgB_{12}H_{12}$ and $CaB_{12}H_{12}$ firstly release hydrogen to form H-deficient $MB_{12}H_{12-x}$ with the icosahedral B_{12} skeletons, followed by a polymerization process to produce $(MB_yH_z)_n$. The anhydrous $MgB_{12}H_{12}$ is amorphous and it decomposes into amorphous boron at 800 °C, whereas $CaB_{12}H_{12}$ may require much higher temperature to complete the decomposition. The lower electronegativity of Ca than that of Mg is considered to be responsible for the higher stability of $CaB_{12}H_{12}$ than that of $MgB_{12}H_{12}$.[36] On the other hand, thermal decomposition of the synthesized $MgB_{12}H_{12}$ and $CaB_{12}H_{12}$ does not seem to be directly correlated with the dehydrogenation of $Mg(BH_4)_2$ and $Ca(BH_4)_2$, suggesting the great importance of further investigation on the correlation between decomposition of possible dehydrogenation intermediates and of the corresponding metal borohydrides.

Acknowledgements

Notes and references

1 S.-i. Orimo, Y. Nakamori, J. R. Eliseo, A. Züttel and C. M. Jensen, *Chem. Rev.*, 2007, **107**, 4111–4132.

2 H.-W. Li, Y. Yan, S.-i. Orimo, A. Züttel and C. M. Jensen, *Energies*, 2011, **4**, 185–214.

3 L. H. Rude, T. K. Nielsen, D. B. Ravnsbaek, U. Bösenberg, M. B. Ley, B. Richter, L. M. Arnbjerg, M. Dornheim, Y. Filinchuk, F. Besenbacher and a. T. R. Jensen, *Phys. Status Solidi A*, 2011, **208**, 1754–1773.

4 H.-W. Li, J. Wang and P. Chen, *MRS Bull.*, 2013, **38**, 480–487.

5 S.-i. Orimo, Y. Nakamori, N. Ohba, K. Miwa, M. Aoki, S.-i. Towata and A. Zuttel, *Appl. Phys. Lett.*, 2006, **89**, 021920.

6 N. Ohba, K. Miwa, M. Aoki, T. Noritake, S.-i. Towata, Y. Nakamori, S.-i. Orimo and A. Züttel, *Phys. Rev. B: Condens. Matter*, 2006, **74**, 075110.

7 H.-W. Li, K. Kikuchi, Y. Nakamori, N. Ohba, K. Miwa, S. Towata and S. Orimo, *Acta Mater.*, 2008, **56**, 1342–1347.

8 S.-J. Hwang, R. C. Bowman, J. W. Reiter, J. Rijssenbeek, G. L. Soloveichik, J.-C. Zhao, H. Kabbour and C. C. Ahn, *J. Phys. Chem. C*, 2008, **112**, 3164–3169.

9 V. Ozolins, E. Majzoub and C. Wolverton, *J. Am. Chem. Soc.*, 2009, **131**, 230–237.

10 C. Bonatto Minella, S. Garroni, D. Olid, F. Teixidor, C. Pistidda, I. Lindemann, O. Gutfleisch, M. D. Baró, R. d. Bormann and T. Klassen, *J. Phys. Chem. C*, 2011, **115**, 18010–18014.

11 Y. Yan, H.-W. Li, H. Maekawa, K. Miwa, S.-i. Towata and S.-i. Orimo, *J. Phys. Chem. C*, 2011, **115**, 19419–19423.

12 M. P. Pitt, M. Paskevicius, D. H. Brown, D. A. Sheppard and C. E. Buckley, *J. Am. Chem. Soc.*, 2013, **135**, 6930–6941.

13 M. Chong, A. Karkamkar, T. Autrey, S.-i. Orimo, S. Jalisatgi and C. M. Jensen, *Chem. Commun.*, 2011, **47**, 1330–1332.

14 Y. Yan, A. Remhof, D. Rentsch and A. Züttel, *Chem. Commun.*, 2015, **51**, 700–702.

15 M. Riktor, M. Sørby, J. Muller, E. Bardají, M. Fichtner and B. Hauback, *J. Alloys Compd.*, 2015, **632**, 800–804.

16 Y. Yan, A. Remhof, D. Rentsch, A. Züttel, S. Giri and P. Jena, *Chem. Commun.*, 2015, **51**, 11008–11011.

17 G. Xia, Q. Meng, Z. Guo, Q. Gu, H. Liu, Z. Liu and X. Yu, *Acta Mater.*, 2013, **61**, 6882–6893.

18 H.-W. Li, T. Matsunaga, Y. Yan, H. Maekawa, M. Ishikiriyama and S.-i. Orimo, *J. Alloys Compd.*, 2010, **505**, 654–656.

19 Y. Kim, S.-J. Hwang, J.-H. Shim, Y.-S. Lee, H. N. Han and Y. W. Cho, *J. Phys. Chem. C*, 2012, **116**, 4330–4334.

20 H.-W. Li, E. Akiba and S.-i. Orimo, *J. Alloys Compd.*, 2013, **580**, S292–S295.

21 C. B. Minella, C. Pistidda, S. Garroni, P. Nolis, M. D. Baró, O. Gutfleisch, T. Klassen, R. d. Bormann and M. Dornheim, *J. Phys. Chem. C*, 2013, **117**, 3846–3852.

22 I. B. Sivaev, V. I. Bregadze and S. Sjöberg, *Collect. Czech. Chem. Commun.*, 2002, **67**, 679–727.

23 J.-H. Her, W. Zhou, V. Stavila, C. M. Brown and T. J. Udovic, *J. Phys. Chem. C*, 2009, **113**, 11187–11189.

24 X. Chen, Y.-H. Liu, A.-M. Alexander, J. C. Gallucci, S.-J. Hwang, H. K. Lingam, Z. Huang, C. Wang, H. Li, Q. Zhao, U. S. Ozkan, S. G. Shore and J.-C. Zhao, *Chem. – Eur. J.*, 2014, **20**, 7325–7333.

25 L. He, H.-W. Li, S.-J. Hwang and E. Akiba, *J. Phys. Chem. C*, 2014, **118**, 6084–6089.

26 V. Ban, A. V. Soloninin, A. V. Skripov, J. Hadermann, A. Abakumov and Y. Filinchuk, *J. Phys. Chem. C*, 2014, **118**, 23402–23408.

27 A. D. Kulkarni, L.-L. Wang, D. D. Johnson, D. S. Sholl and J. K. Johnson, *J. Phys. Chem. C*, 2010, **114**, 14601–14605.

28 V. Stavila, J.-H. Her, W. Zhou, S.-J. Hwang, C. Kim, L. A. M. Ottley and T. J. Udovic, *J. Solid State Chem.*, 2010, **183**, 1133–1140.

29 N. Nogi and S. Tanaka, *J. Solid State Chem.*, 2006, **179**, 2927–2933.

30 S. Hermanek, *Chem. Rev.*, 1992, **92**, 325–362.

31 S.-J. Hwang, R. C. Bowman Jr., C. Kim, J. A. Zan and J. W. Reiter, *J. Anal. Sci. Technol.*, 2011, **2**, A159–A162.

32 Y. Yan, A. Remhof, S.-J. Hwang, H.-W. Li, P. Mauron, S.-i. Orimo and A. Züttel, *Phys. Chem. Chem. Phys.*, 2012, **14**, 6514–6519.

33 A. Remhof, Y. Yan, D. Rentsch, A. Borgschulte, C. M. Jensen and A. Züttel, *J. Mater. Chem. A*, 2014, **2**, 7244–7249.

34 H.-W. Li, K. Kikuchi, T. Sato, Y. Nakamori, N. Ohba, M. Aoki, K. Miwa, S.-i. Towata and S.-i. Orimo, *Mater. Trans.*, 2008, **49**, 2224–2228.

35 Y. Kim, D. Reed, Y.-S. Lee, J. Y. Lee, J.-H. Shim, D. Book and Y. W. Cho, *J. Phys. Chem. C*, 2009, **113**, 5865–5871.

36 Y. Nakamori, K. Miwa, A. Ninomiya, H. Li, N. Ohba, S.-i. Towata, A. Züttel and S.-i. Orimo, *Phys. Rev. B: Condens. Matter*, 2006, **74**, 045126.